Journal of Molecular Liquids 350 (2022) 118551

Contents lists available at ScienceDirect

Journal of Molecular Liquids

journal homepage: www.elsevier.com/locate/molliq

Betaine-urea deep eutectic solvent improves imipenem antibiotic activity

Belén Olivares [a,b,*,1], Fabián A. Martínez [c,1], Marcelo Ezquer [d], Bernardo J. Morales [e], Ignacia Fuentes [f,g], Margarita Calvo [h,i], Paola R. Campodónico [a]

[a] Universidad del Desarrollo, Instituto de Ciencias e Innovación en Medicina, Centro de Química Médica, Santiago, Chile
[b] Universidad Nacional de Cuyo, Programa de Doctorado en Biología, Mendoza, Argentina
[c] Universidad de Santiago de Chile, Laboratorio de Resonancia Magnética Nuclear, Santiago, Chile
[d] Universidad del Desarrollo, Instituto de Ciencias e Innovación en Medicina, Centro de Medicina Regenerativa, Santiago, Chile
[e] Universidad Pedro de Valdivia, Facultad de Ciencias de la Salud, Santiago, Chile
[f] DEBRA Chile, Santiago, Chile
[g] Universidad del Desarrollo, Centro de Genética y Genómica, Facultad de Medicina, Santiago, Chile
[h] Pontificia Universidad Católica de Chile. Facultad de Ciencias Biológicas, Santiago, Chile
[i] Millennium Nucleus for the Study of Pain (MiNuSPain), Chile

ARTICLE INFO

Article history:
Received 10 October 2021
Revised 18 December 2021
Accepted 14 January 2022
Available online 19 January 2022

Keywords:
Betaine-urea
Antibiotic stability
NADES toxicity

ABSTRACT

Beta-lactam antibiotics are highly unstable in aqueous media, which may lead to subclinical concentrations, antimicrobial resistance and therapeutic failure. In previous work we demonstrated that a natural deep eutectic solvent consisting of betaine and urea (BU) is capable of improving the stability of some beta-lactams, including imipenem (IMP), the most unstable antibiotic of the family. Here, IMP-BU was studied by selective protonic Nuclear Overhauser Effect Spectroscopy Magnetic Resonance (H^1 NOESY NMR) to gain insight into the mechanism by which BU protects IMP. The kinetics of IMP release and its antibacterial activity were evaluated in diffusional, time-kill and antibiofilm assays. It was found that BU is a protective matrix which allows a fast release of IMP, resulting in superior antibacterial activity when compared to IMP in aqueous solution, both against bacteria growing in planktonic form and in biofilms. Furthermore, it was shown that BU is nontoxic when evaluated in fibroblast primary cell cultures and in organotypic skin cultures, and is not immunogenic when tested *in vitro* in macrophage cultures, suggesting that BU has potential application as a biomaterial or excipient.

1. Introduction

Antibiotics are a precious resource without which we could not conceive a vast number of health care practices. However, we are experiencing a pronounced antibiotic shortage crisis due to the accelerated emergence of antimicrobial resistance to existing antibiotic molecules, which is not being counteracted by the development of new antibiotics.

The World Health Organization and the World Bank have stated that infections by resistant pathogens are a threat to our global health and economic future, estimating an annual loss of 3.8 % of the global gross domestic product (GDP) by 2050 [1].

Antibacterial efficacy and antibacterial resistance mechanisms rely heavily on the accurate management of the pharmacokinetics and pharmacodynamics parameters of the specific antibiotic molecule [2]. Clinicians are highly focused on the refinement of every single step of antibiotic therapy, aiming to provide the right concentration at the desired site of action and during the right time of exposure, in order to avoid therapeutic failure and prevent antibiotic resistance. Also, many *in silico* tools have been implemented during recent years to optimize antibiotic treatments [3] and to repurpose old antibiotics.

Beta-lactam antibiotics are old drugs but remain the most successful antibiotic class for the majority of bacterial strains [4]. Therefore, many strategies are being continuously applied to maintain their usefulness. For example, in the investigational field, they have been combined with adjuvant compounds, such as potentiators and inhibitors of specific clearance molecules in the biochemical route of antibiotic resistance [5 6]. In the clinical field, considering that the efficacy of this group of

* Corresponding author at: Centro de Química Médica, Instituto de Ciencias e Innovación en Medicina, Facultad de Medicina, Universidad del Desarrollo, Santiago, Chile.
E-mail address: molivares@udd.cl (B. Olivares).
[1] # Belén Olivares and Fabián A. Martínez contributed equaly to this work.

https://doi.org/10.1016/j.molliq.2022.118551
0167-7322/

antibiotics is time dependent and their clinical success depends on the time its concentration remains above the minimal inhibitory concentration [7], many strategies have been implemented to achieve this goal, such as continuous infusion or coadministration with drugs that inhibit their clearance. However, these two strategies have some limitations: the inherent low physicochemical stability of beta-lactams, and a higher probability of adverse reactions, respectively [8]. With the purpose of improving efficacy, many extended release formulations have been developed, and some of them have demonstrated better clinical outcomes avoiding pharmacokinetics and anatomical challenges, such as amoxicillin-clavulanate and azithromycin, among others [9 10]. Nevertheless, to our knowledge, extended release formulations have not been developed for carbapenems, the most unstable of the beta-lactam molecules. Carbapenems constitute a valuable group of beta-lactams, being the best therapeutic option in many severe infections, with the best outcomes in terms of survival and bacteriologic clearance in critical clinical situations [11].

In our previous work, a new solvent formulation based on a deep eutectic solvent composed of betaine:urea (BU) was designed to enhance the stability of imipenem [12], which is the most unstable beta-lactam antibiotic molecule. The aim of the present work was to evaluate if the enhanced stability attained with the new formulation correlates with an improvement in effectiveness, evaluating the antibacterial activity, the type of kinetics involved during the release of IMP, and to ascertain how the BU components interact with the drug to envision a possible mechanism of stabilization. Furthermore, the biocompatibility of BU was also evaluated.

2. Materials and methods

2.1. Drugs and reagents

Imipenem monohydrate (IMP) (USP Cat. N 1337809, Sigma-Aldrich). For the preparation of BU solvent, 98% betaine monohydrate (Santa Cruz Biotechnology) and 98% urea (Merck) were used. Ultrapure water was obtained with a Simplicity® (Millipore) purification system.

2.2. Preparation of BU solvent

BU was prepared by the heating-mixing method, since natural deep eutectic solvents (NADES) containing a known amount of water may be obtained with this method [13]. BU was prepared in the formulation B:U:W 1:1.5:1.25, where the final concentration of water was 9.8 % w/w, considering the water in the betaine reagent and the 2 % added. Briefly, betaine and urea were placed in a closed round bottom flask at a1:1.5 M ratio, and heated in a water bath at 60 °C with agitation (200 rpm) for 2 h until a clear liquid was obtained. Water was added at 2 % w/w, leading to a final molar ratio composition which has been shown to be stable [12] Additionally, for IMP stability assays, preparations with 5 % and 15 % w/w of added water were obtained, leading to B:U:W formulations of 1:1.5:1.63 and 1:1.5:2.88.

2.3. Viscosity and water measurements

Dynamic viscosity was measured at 25 °C and 37 °C using a rotational viscometer (Fungilab Viscolead series) connected to a circulating water bath. Water titration was performed using an 831 KF Coulometer Metrohm®.

2.4. Stability of IMP in BU formulations with different water contents

A solution of IMP in water and in the B:U:W formulations of 1:1.5:1.25, 1:1.5:1.63 and 1:1.5:2.88 were prepared by mixing the solvent and solutes for 20 min using a vortex, and the resulting mixtures were kept at 25 °C +/- 2 °C for five days in a water bath circulation system (PolyScience, USA). Samples were taken at 0, 1, 2 and 5 days and analyzed by high performance liquid chromatography (HPLC) as previously reported [12]. Quantitations were made considering the areas of the chromatographic peaks applying the following formula:

$$\%remainingdrug = \frac{Area_t}{Area_0} \times 100$$

2.5. Imipenem release

IMP was dissolved in BU by gently mixing the drug powder with the liquid BU. Before starting the release experiment, the IMP-BU mixture was allowed to reach equilibrium at room temperature for 24 h.

Release of the drug was monitored in a diffusion experiment. Samples containing 250 µl of 1 mg/ml BU-IMP were placed in a bicameral device consisting of a well plate with inserts (8 µm pore) used as permeable support (Transwell®). Five independent samples were allowed to diffuse from the upper compartment to the lower compartment containing 1 ml of physiological phosphate buffer pH 7,4. The system was kept at 37 °C, in agitation (200 rpm) for 24 h. Samples of 100 µl were withdrawn from the lower compartment at nine time intervals (0, 10, 20, 30, 40, 60, 120, 180, 360 and 1440 min), while maintaining sink conditions adding the same volume of preheated buffer. The IMP content was measured using a high-performance liquid chromatography method previously developed in our laboratory [12].

Kinetics of release: in order to understand the kinetics associated to the release of IMP from BU, the semi-empirical model of Peppas-Korsmeyer [14,15] was used applying the formula

$$\frac{M_t}{M_\infty} = Kt^n$$

where M_t is the quantity of drug released at time t, $M\infty$ is the quantity of drug released at equilibrium. Constants k and n are characteristic of the solvent-polymer system. The n constant is the diffusional parameter and depends on the geometry of the device and on the mechanism of physical transport of the solute. Parameter k incorporates BU characteristics of the system. Additionally, the Hixon-Crowel model was applied [16] according to the formula:

$$Wt^{1/3} = W_0^{1/3} - K_{HC}t$$

where Wt is the amount of drug remaining at time t, W_0 is the initial amount of drug (at time t = 0), and K_{HC} represents the dissolution rate constant. Data were fit to the equation obtaining a plot of the cubic root of the unreleased fraction of the drug ($W_0^{1/3}$ - $Wt^{1/3}$) versus time.

2.6. Nuclear Overhauser effect Spectroscopy Magnetic Resonance (NOESY NMR)

Selective NOESY NMR measurements were recorded on a Bruker Advance NEO 400 spectrometer (Bellerica, MA, USA) operating at 400.13 MHz (^{1}H) and 100.62 MHz (^{13}C) at 27 °C. All samples were prepared containing 100 µl of deuterated water to perform solvent tuning. Selective NOESY was performed by integrating those signals that did not show overlap. Each experiment was carried out by varying the mixing time parameter (D8) in a range of

0.2 to 1.0 s in order to study the rigidity of the system and the speed by which the transfer of magnetization occurs. The $^{1}H–^{1}H$ NOESY and $^{1}H–^{1}H$ ROESY (Rotating frame Overhauser Effect Spectroscopy) experiments were carried out once the best mixing time was determined.

2.7. Microbiological sensitivity assays

2.7.1. Time kill assay

An inoculum of *Pseudomonas aeruginosa* (ATCC-27853 strain) was adjusted to 0.5 McFarland turbidity from a fresh overnight growing broth, and then diluted to 1×10^6 CFU/ml in Mueller Hinton broth. One milliliter of this suspension was incubated at 37 °C with agitation (200 rpm). Each well of a 24 well-plate was fitted with diffusion inserts (Transwell® 8 μm pore) and 100 μl of either BU-IMP (1 μg/ml), IMP (aqueous) (1 μg/ml) or Urea/Betaine (47.2/61.4 mg/ml) were placed on the inserts. Samples of the liquid culture were withdrawn at 6 and 24 h and bacteria were counted by flow cytometry. Briefly, 50 μl samples were diluted three logs in PBS and stained with SYTO BC® green/propidium iodide (fluorescent nucleic acid stains) with the addition of fluorescent beads and data were acquired in a Cyan Dako cytometer.

Stability analyses of imipenem under the killing test conditions were performed in a parallel plate incubated under the same conditions. Samples of the medium were taken at ten minutes, and 2, 4, 6, 8 and 24 h of incubation, filtered through 0.22 μm membrane filters and 50 μl aliquots were injected into the HPLC system as previously reported [12].

2.7.2. Anti biofilm assay

P. aeruginosa biofilms were grown on a collagen gel matrix as previously described [17] with some modifications. Briefly, 50 μl of collagen gel were prepared in a 96 well plate by mixing a 3 mg/ml solution of rat-tail tendon collagen (Sigma-Aldrich) in PBS buffer with a 0.1 N sodium hydroxide solution to achieve crosslinking. The collagen matrix obtained was inoculated with 25 μl of a *P. aeruginosa* suspension adjusted to 1×10^6 CFU/ml in LB broth and incubated 24 h at 37 °C. Six replicates of 24-hour biofilms were then treated with 50 μl of i) IMP-BU, ii) 32 μg/ml IMP (aqueous solution), iii) 47.2 mg/ml betaine and 61,4 mg/ml urea, and iv) PBS (control) for 24 h. Bacterial counting was performed by flow cytometry of stained live and dead bacteria using 1 μl SytoBC® and 1 μl propidium iodide, after dispersal of the biofilm by incubating the collagen matrix in a 500 μg/ml collagenase solution (Gibco® Collagenase Type I) for 90 min at 37 °C, with vortexing every 30 min as previously reported [18].

2.8. BU biocompatibility

2.8.1. Cytotoxicity assays

The BU cytotoxicity was evaluated *in vitro* using ATCC® Normal Human Primary Dermal Fibroblasts from neonatal foreskin. Cells were cultured in DMEM (Dulbecco's modified Eagle's medium, Lonza, Belgium) supplemented with 10% heat-inactivated FBS (fetal bovine serum, Gibco, UK) and maintained in T-flasks incubated in a humidified atmosphere with 5% CO_2 at 37 °C. 5×10^4 cells were seeded in 500 μl-well plates until they reached confluency. Their viability was then examined indirectly throughout 24 h of exposure to different concentrations of BU with the CellTiter-Blue® (Promega) mitochondrial function assay following the manufacturer's instructions.

2.8.2. Immunogenicity test

The BU immunogenicity was evaluated *in vitro* using the human monocyte cell line THP-1. For this, 4×10^5 THP-1 cells were cultured in 24-well plates under previously reported conditions [19]. Cells were differentiated to a macrophage phenotype by adding 25 nM of phorbol 12-myristate 13-acetate (PMA), incubating for 48 h and then for an additional 24 h in fresh complete medium. Once the phenotype changed to that of adherent cells, they were activated by incubation with lipopolysaccharide (LPS) at 0.01 and 1 μg/ml for 24 h (positive control), or with 0.96 and 2.1 mg/ml BU doses. Total RNA was then purified using Trizol (Invitrogen). One microgram of total RNA was used to perform reverse transcription with MMLV reverse transcriptase (Invitrogen) and oligo dT primers. Real-time PCR reactions were performed to amplify the cDNA of pro-inflammatory cytokines IL6, IL8 and TNF-α using a Light-Cycler 1.5 thermocycler (Roche, Indianapolis, IN) as previously reported [20]. Relative quantifications were performed by the ΔΔCT method. Data were normalized against the housekeeping gene GAPDH and expressed as folds change compared to control (untreated) cells.

2.8.3. Human skin explants

Human skin explants were generated from fresh skin obtained from patients undergoing elective cosmetic surgery who signed a written informed consent (Protocol N° 171002003, PUC Ethics Committee). The skin of one donor was cleaned from underlying fat, and full-thickness skin sections were obtained with a 6 mm biopsy punch as previously reported [21]. Skin pieces were cultured in a dermal-side down position using a Transwell® (8 μm pore) insert as tissue support allowing contact with 500 μl of culture medium in 24-well plates, while the epidermis remained above the medium/air interface. The culture medium, which consisted of DMEM (Sigma Aldrich) supplemented with 10% FBS, 0.2% gentamicin and 0.2% Primocin®, was maintained at 37 °C in a humidified atmosphere of 5% CO_2. 50 μl of BU were applied on the epidermis explants, while a control group was treated with PBS. However, given that the test samples are liquid, they also came into direct contact with the sub epidermis tissue. Cultures were maintained for 24 and 48 h. Sample sections were then fixed in 4% paraformaldehyde, embedded in paraffin, cut to a thickness of four microns and stained with hematoxylin and eosin. Signs of damage were evaluated and ranked in a severity score of 0 (not present) to 4 (markedly present) by a specialized pathologist. The statistical analysis was made using the paired two tailed Wilcoxon signed rank test. A $p < 0.05$ was considered significant.

2.9. Statistical analyses

Statistical analyses were performed using GraphPad Prism (San Diego, CA). Data are expressed as means ± SEM. The normal distribution verification was tested using the Shapiro–Wilk test. For normally distributed data, one-way or two-way analysis of variance (ANOVA) was used followed by a Fisher post test. When only two groups were compared, statistical significance was determined by Student's *t*-test. A $p < 0.05$ was considered indicative of statistical significance.

3. Results and discussion

3.1. IMP stability is diminished by water content

BU is a network resulting from strong hydrogen bonds between betaine and urea, with a dynamic viscosity of 41.04 mPa.s at 25 °C and 17.21 mPa.s at 37 °C.

In our previous work we analyzed the effect of water content in the continuity of the BU network by ^{1}H NMR and ^{13}C NMR. We reported that, with increasing water content, a disruption in the betaine-urea engagement is accompanied by an increase in the dynamic behavior of the molecules and a decrease in viscosity

[12]. Consequently, it is expected that the higher the dynamic behaviour of urea and water molecules, the higher their nucleophilic character, affecting IMP stability. This is in agreement with the effect observed in the stability assay shown in Fig. 1. As the water content of the B:U:W formulation increases from 1.25 to 1.63 to 2.88, the amount of IMP remaining on the fifth day is increasingly less, 73 (SEM ± 0.36), 55 (SEM ± 1.0) and 50 (SEM ± 0.07) % w/w of the initial drug concentration respectively.

3.2. The release of imipenem from BU is a Case II type process

BU could be consider a noncovalent or supramolecular polymer resulting from the network of strong hydrogen bonds between betaine and urea [22]. Given its potential as a novel solvent system for an antibiotic it is of interest to study the mechanism by which the drug is released from the BU matrix. With that purpose, we evaluated the kinetics of the release of IMP from the BU matrix using a vertical diffusion cell system, which is the most recommended approach for viscous fluids [23 24].

Fig. 2A depicts the concentration versus time profile obtained. Data were fit to the Peppas-Korsmeyer equation (Fig. 2B) from which a diffusion constant that indicates the type of kinetic release may be calculated [14]. We chose this model because it is a general one, applicable to a vast number of matrices and solute types, and especially because it does not assume concentration dependencies. To our knowledge, this is the first time that the release of a drug from a NADES is described, so the Peppas-Korsmeyer model is suitable as a first approach to elucidate if the IMP release from BU follows a Fickian or non-Fickian diffusion model.

The extent and rate of release of a drug are considered a combination of diffusion and Case II transport of drug molecules through the matrix they are inserted in. Diffusion is governed by Fick's law while Case II transport reflects the influence of polymer relaxation on the movement of the matrix molecules [25]. At the same time, drug transport is an overall dynamic process which follows a series of staged processes during release. At time zero, the external buffer causes a counter current flow, during which the drug migrates from the interior to the exterior of the BU matrix. It is during this first stage that the greatest release of the drug is observed (Fig. 1A). In fact, the release starts to reach equilibrium after the first hour of experimentation. The diffusional constant value of 1.16, obtained through the Peppas Korsmeyer equation, indicates that, in this system, the release of IMP behaves as a Case II transport. This type of transport is characterized by a sharp diffusion front, in which the penetrating buffer substantially swells the polymer [26]. Hence, the release could be taking place while the BU microstructure suffers a disentanglement and erosion by the water molecules. The high diffusional constant value suggests that the release of IMP involves multiple processes, with a mechanism of relaxation of the noncovalent chains and the breaking of the matrix being predominant. Thus, it turns out that the release mechanism is mostly driven by a process of erosion controlled by the surrounding solvent molecules, and the material loss of the bulk of the matrix.

Additionally, the analysis based on the Hixson-Crowell model, capable of elucidating if the release depends on the shape parameters of the matrix rather than corresponding to a Fickian diffusion process [27] , had a high coefficient of determination R^2 (Fig. 2C). This goodness of fit to the model supports a release mechanism mostly based on the morphology or shape and thus reinforces the Case II type release obtained with the Peppas Korsmeyer model.

Another important aspect of BU is that it constitutes a completely biodegradable and bioerodible system, without enzymatic action needed. This sets a big difference when compared to other covalent urea inclusion systems such as nonbiodegradable polyurethanes [28].

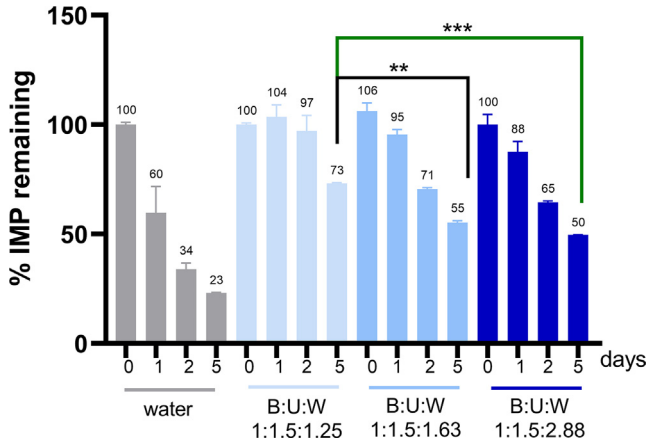

Fig. 1. Stability of imipenem in BU formulations having different water content. The concentration of the remaining drug was determined by HPLC. Data are presented as the mean ± SEM of three independent replicates. Significant differences between formulations differing in their water content were observed on the fifth day as determined with a one-way ANOVA test.

3.3. Imipenem is preferentially solvated by betaine

NOESY is a nonroutine technique which represents a useful strategy that takes advantage of viscous solvents to perform analyses of solutes in the mixture [29 30]. Thus, as BU represents a viscous solvent for IMP, we applied this technique to analyze a possible solvation arrangement.

NOESY experiments usually require prior study of the system to be characterized. Among the most important parameters to be optimized is the mixing time (D8). This parameter refers to the speed by which the transfer of magnetization occurs through space. A fast transfer and small D8 value is related to a system where mobility is low and therefore relaxation becomes efficient. Conversely, a system in which a large D8 is required implies that the excited groups must take more time to meet spatially before energy transfer can take place. Thus, large D8 values correlate with highly mobile systems, in which there is not efficient energy transfer between the excited groups. Usually, the mixing times used in NOESY experiments range from 0.1 to 1.0 s. To have a clear certainty of the best mixing parameter, a sweep in the recommended range of D8 was carried out to establish how mobile the system is, to set the best response to the interaction. In order to obtain a truthful answer against possible magnetization transfers, selective NOESY experiments were carried out. In this way, it is possible to minimize the errors that may be introduced by the high concentration of the BU components compared to the concentration of the drug. A selective experiment allows the excitation of specific protons in the sample, resulting in that only those protons which they interact with, giving them magnetization, appear in the spectrum.

During the modification of the D8 parameter, it was found that the best magnetization transfer responses occur at D8 of<0.6 s. These results can be explained by the strong hydrogen bonding interactions generated between betaine and urea. In other words, the drug molecules dissolve in BU and become trapped within the compact matrix. Thus, when a proton of the drug is excited, it can quickly deliver this energy to betaine or urea.

The spectrum of the selective NOESY NMR experiment of IMP dissolved in BU (Fig. 2) indicates that there is a preferential energy exchange between the protons of the IMP methyl groups and the protons of the betaine methyl and methylene groups. This finding is related to the closeness of betaine to IMP in a possible solvation arrangement. The spectrum also shows urea protons, receiving magnetization energy from IMP decay, but conversely the energy

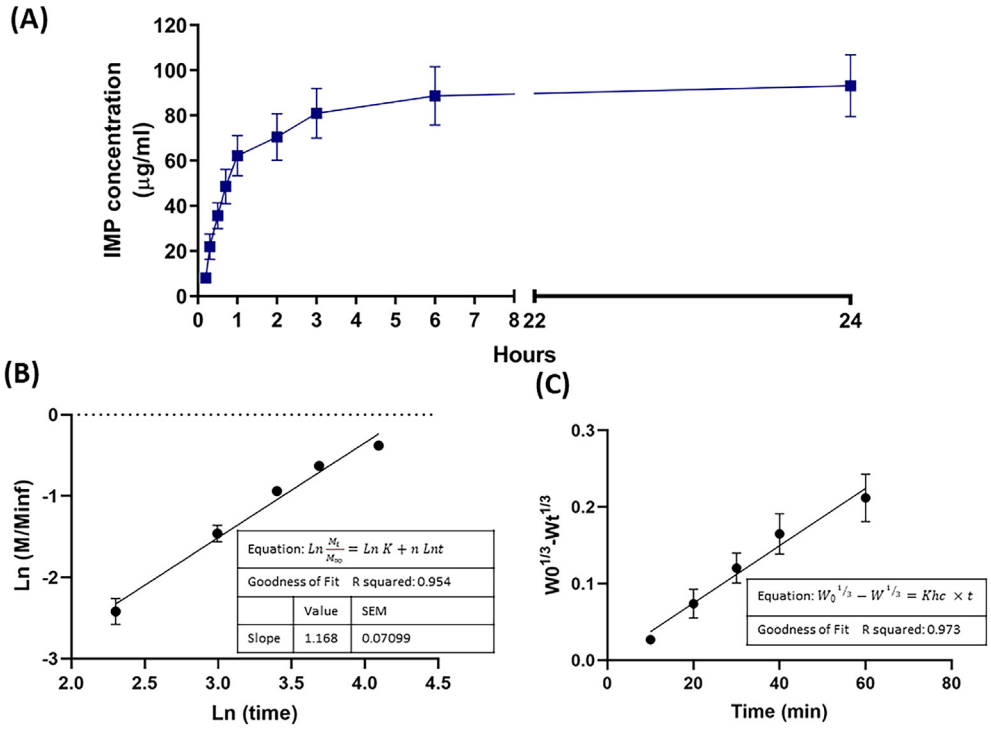

Fig. 2. A) Cumulative profile of IMP released from a BU matrix containing 1 mg/ml of IMP. Concentrations in the bathing medium were determined by HPLC. Data are presented as the mean ± SEM of three replicates. **B) Analysis of the release process according to the Peppas Korsmeyer equation**. The data fit a line where the slope corresponds to the n diffusional constant. **C) Analysis of the release process according to the Hixson-Crowel equation**. The coefficient of determination R^2 indicates the goodness of fit to the model.

interchange is of a lower magnitude. Fig. 2A shows that as the mixing time D8 increases, the intensity of the signals is lost. This phenomenon denotes that the system relaxes quickly through energy transfer, which is characteristic of a rigid system. In other words, the hydrogen bonding interactions generate a compact matrix, where the closeness of the molecules allows the rapid relaxation of the system. Fig. 2B shows the NOESY spectrum obtained using a D8 of 0.2 s. The interactions with the protons of betaine (3.9 and 3.3 ppm) and urea (6.0 ppm) are clearly observed. The signal corresponding to the interaction with urea is less intense, which denotes a lower preference compared to betaine.

Something interesting that should be highlighted is that when studying the urea signal, a tremendously strong association was found with the deuterated water used as solvent to do the tuning. This can be confirmed by observing that when the excitation of the urea signal occurs, so does the deuterated water signal and vice versa. It should be mentioned that both signals do not appear in the same range of chemical displacement, discarding an overlapping effect. This event seems to be more closely related to an enormous affinity between the two molecules, preventing urea and water from interacting with imipenem. In fact, when deuterated water is excited, it does not present any interaction with the IMP molecules.

3.4. IMP-BU shows enhanced antimicrobial activity towards planktonic bacteria

The antibiotic activity test chosen to evaluate the antimicrobial activity of IMP-BU was a time kill assay based on a growing inoculum of planktonic *P. aeruginosa*. In it, a dynamic condition allows the *in vitro* antimicrobial activity to be evaluated considering the multivariate kinetic changes: antibiotic concentration, IMP release and bacterial growth in a shaking broth at 37 °C h. The IMP dose of 1 µg/ml was the MIC determined previously in a sensitivity test of microdilution, a static condition, for the same microorganism (data not shown). This drug concentration was not inhibitory under the killing dynamic condition, which was evident in the bacterial count profile shown in Fig. 3A. These results are in agreement with those reported previously for *P. aeruginosa* with the same antibiotic dose [27]. Fig. 3A also indicates that the IMP-BU formulation is superior in its antibacterial activity when compared to IMP in aqueous solution, throughout the entire evaluation period, showing a significant reduction in the living bacterial count after 6 and 24 h of exposure. This finding is probably related to the BU capacity to continue releasing fresh antibiotic molecules from its protective matrix to the broth medium, leading to longer exposure to the antibiotic. Fig. 3B depicts the concentration of remaining IMP throughout the test. It can be seen that IMP-BU takes an hour to reach total drug concentration exposure, in accordance with the delivery profile determined previously (section 3.1). Then, the drug concentration drops at the end of the experiment because of the progressive disassembling of BU and the progressive contact with the threatening medium conditions. Thus, the encapsulated IMP-BU gives higher levels of drug while the BU matrix remains assembled, allowing the preferential protective solvation by betaine molecules, as was observed through the selective NOESY experiments (section 3.3). Indeed, there were no reductions in the IMP concentration up to four hours after IMP-BU treatment (two-way ANOVA, $p > 0.05$), while it does diminish significantly from the beginning when dissolved in aqueous solution (two-way ANOVA, $p < 0.05$).

The evidence of IMP instability concomitant with the loss of activity, has been previously reported in the same broth medium [31 32], in serum during *in vitro* studies [33] and *in vivo* when evaluated during pharmacokinetics studies. Moreover, *in vivo* reports recognize that there is an extra renal drug clearance effect mediated by the IMP instability phenomenon, leading to antibiotic effectiveness being inferior to that expected [34].

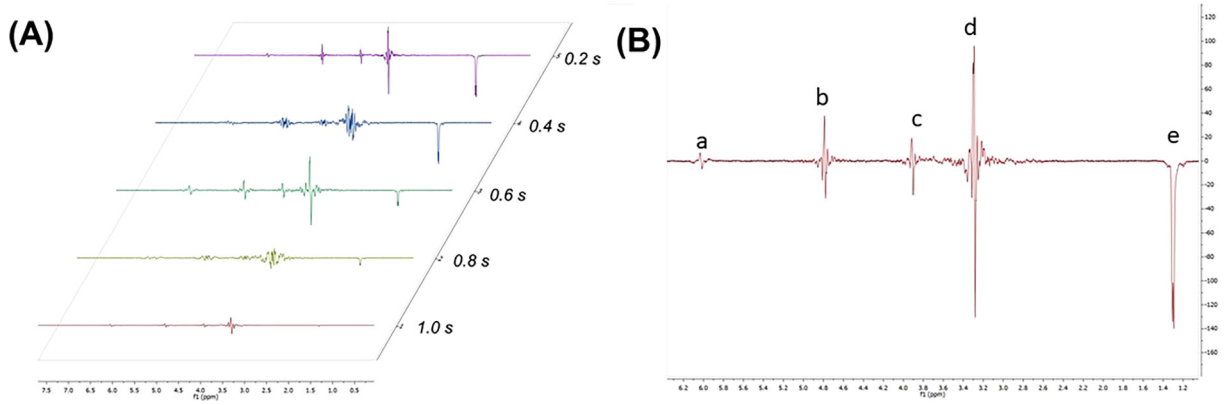

Fig. 3. (**A**) **Variation of the D8 parameter on the NOE for the IMP methyl groups** (**B) Protonic NOESY selective spectrum for the methyl groups of IMP**. Data were recorded using a D8 of 0.2 s. Signals of a) urea, b) deuterated water, c) betaine methyl groups, d) betaine methylene groups, and e) IMP methyl group pulses.

3.5. IMP-BU shows enhanced antibiofilm activity

Bacteria growing in biofilms represent one of the most challenging conditions for antimicrobial activity [35]. Biofilms have additional mechanisms that lead bacteria to tolerate high drug doses. The biofilm mode of growing represents a challenging condition, both for the time that the nondegraded drug must be present at the site of bacterial growth, and for the capacity of the antibiotic molecules to penetrate the biofilm matrix to reach the bacteria. Those mechanisms result in a large part of the biofilm cells being able to escape from the attack of both antibiotics drugs and the immune system [35]. In this context, our comparative antimicrobial experiment considered the maximum dose of the specified compendial range for imipenem sensitivity testing [36], which is exposure of a 24 h mature *P. aeruginosa* biofilm to 32 μg/ml of IMP. The IMP-BU formulation showed superior antibiofilm activity when compared to IMP dissolved in water, exerting a 70% reduction in the viable bacterial count after 24 h of exposure (Fig. 4). The bacterial viability results measured for that same IMP concentration are similar to or slightly higher than those reported by other authors [37], probably because of the use of the collagen fibers matrix, which represents an additional interphase between bacteria and drug. Moreover, the limited access to oxygen turns the intricate biofilm into a more metabolically inactive entity, and thus less susceptible to the action of IMP [38]. However, the higher antibacterial activity of the IMP-BU formulation in this *P. aeruginosa* biofilm system may be explained by the enhanced stability of IMP when is in the protective betaine solvation provided by the BU matrix (see section 3.3) together with BU acting as a permeability enhancement agent. The latter capacity is mainly based on the power of urea to change the properties of the water that surrounds proteins and modify the permeability through the collagen fibers [39 40].

3.6. BU has an IC50 in the molar concentration range and is not immunogenic

The biocompatibility of BU was evaluated in a cytotoxicity test and in an *in vitro* immunogenic test on primary cells in culture. There are many studies on the cytotoxicity of NADES performed in mammalian immortalized cells in culture [41 42], but to our knowledge, this is the first study on primary cell cultures, which can give a more realistic approximation to normal cell metabolism. Primary cultures of human skin fibroblasts were chosen because this cell type is abundant in the conjunctive tissues, relevant for future topical applications. BU was expected to have a good cytotoxic dose index because it is an ammonium based NADES, a class which has been declared of low toxicity compared to phosphonium based counterparts [41]. Surprisingly, however, the calculated IC50 value for BU was 75 mg/ml (95% CI 67.7–84.8) (Fig. 5A), a thousand times higher than that of other ammonium based NADES having choline chloride as the hydrogen acceptor, for which there are reports in the micromolar or millimolar range on immortalized cell lines [43 41,44].

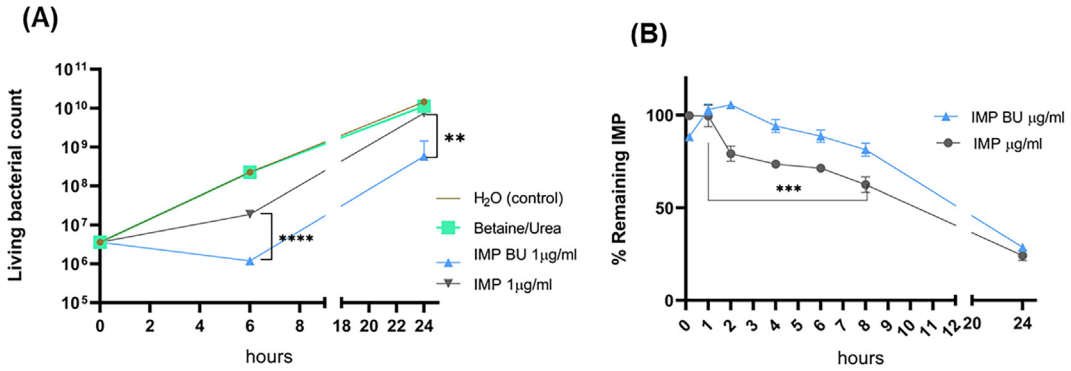

Fig. 4. A) Killing curves of planktonic *Pseudomonas aeruginosa*. Viable bacterial count performed by flow cytometry after SytoBC®/PI staining at 6 and 24 h of incubation with IMP. Data are presented as the mean ± SEM of three independent replicates. A two-way ANOVA test indicated significant differences between IMP-BU (5.8×10^8) and IMP aqueous solution (7.5×10^9). **B) Stability profile of IMP dissolved in water and in BU** in Muller Hinton broth. The levels of remaining IMP were measured by HPLC. Data are presented as the mean ± SEM of three replicates. A two-way ANOVA test indicated significant differences between the concentration of remaining IMP from IMP-BU and IMP aqueous solution during the first 8 h of treatment.

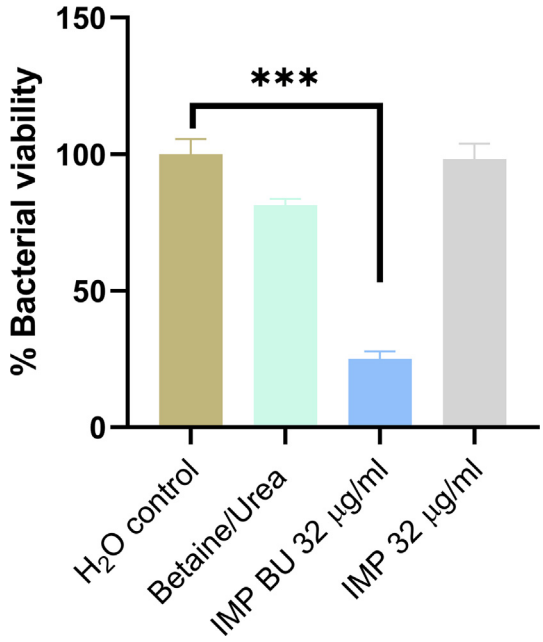

Fig. 5. Bacterial viability in a *P. aeruginosa* biofilm determined by flow cytometry after 24 h of exposure to IMP using SytoBC® and propidium iodide staining. Data are presented as the mean ± SEM of three independent replicates. A one-way ANOVA test indicated significant differences at 24 h of exposure.

On the other hand, the lower cytotoxicity of NADES compared with that of ionic liquids (IL) has been well documented [45,46]. The main reason leading to this observation is the strong cationic nature of IL, which can interact with cell membranes in a surfactant manner [47 48]. Other authors have also referred to this cationic character as the toxicophore in cholinium based NADES when tested in cell lines [41]. Conversely, BU lacks ionic character: in betaine, the hydrogen bond acceptor is a zwitterionic molecule, and urea, the hydrogen bond donor (HBD), is a neutral molecule. Thus, this is probably the main reason for its low toxicity. The same conclusion has been reached by Ventura *et al.*, who have compared the ecotoxicity of zwitterionic versus ionic liquids [49].

Moreover, BU has a reduced toxicity profile when compared to other betaine-NADES bearing acids acting as HBD [44 50]. This may also be related to the nonacidic character of urea, leading to less charge transfer between components. In conclusion, only partial charge interchanges in the hydrogen bond network are present in BU. Thus, this could be the main cause of the good cytotoxic profile observed in our study.

Another important aspect in the biocompatibility evaluation of new materials is their potential to generate an immune response. Based on considerations of BU as a supramolecular polymer that could emulate an immunogenic pattern, we evaluated its immunogenicity in a human macrophage cell culture system. THP-1 cells stimulated by PMA are commonly used to assess the ability of different compounds to modulate macrophage activity through measurements of the induction of the expression of genes encoding inflammatory cytokines [51] . Our results showed no activation after BU exposure compared to the control cells (Fig. 5B). Conversely, incubation of macrophages with LPS, as a classical immunogenic stimulus, induced a robust increase in the mRNA levels of proinflammatory cytokines in a dose dependent way (Fig. 5B).

3.7. BU is nontoxic when applied on an organotypic culture of human skin explants

Finally, in order to get closer to an *in vivo* situation, BU toxicity was evaluated in human skin explants as described in the methods section. This model has been described as the most useful to test biomaterials due to the three dimensional structure of intact skin, allowing the evaluation of cell to BU interactions, while maintaining the cross-communication at the dermis/epidermis interface [52]. Under this *ex vivo* model dermis and epidermis were in contact with BU for 24 and 48 h. As may be seen in Fig. 7, all specimens, including those treated with BU and untreated specimens, maintained a very similar dermal and epidermal architecture at the two times of evaluation, while the histopathological analysis did not find differences ($p > 0.05$) in the signs of damage assessed. These results complement the biocompatibility profile, giving information on the topical effect of BU under a pure, direct and assembled condition of contact with tissue cells.

It has been reported that urea in concentrations above 20% can cause some irritant effects in the skin [53]. However, despite the high urea content in BU (almost 40% w/w), the absence of adverse signs may be explained by the strong betaine urea interaction unveiled during the NMR experiments (see section 3.2 and Fig. 2C), resulting in less availability of free urea.

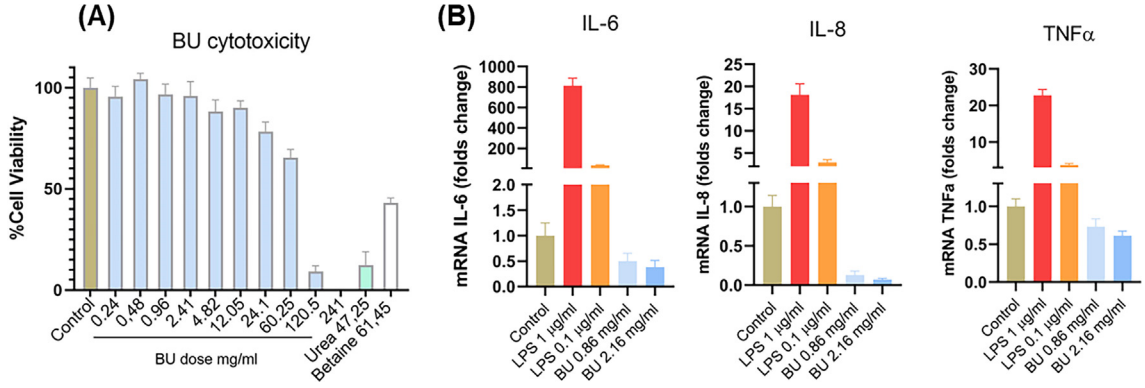

Fig. 6. A): Viability of human dermal fibroblasts after 24 h of exposure assessed by mitochondrial activity determination using Cell Titer Blue®. Data are presented as the mean ± SEM of three independent replicates. **B) Expression of cytokine genes in M1 macrophages derived from THP-1 monocyte cells**. mRNA levels were determined by RT-qPCR of the proinflammatory cytokines IL-6, IL-8 and TNF-α. LPS (1 mg/ml and 0.1 mg/ml) was used as positive control of macrophage activation. Data were normalized against the housekeeping gene GAPDH and expressed as folds change compared to control (untreated) cells. A two-tailed *t*-test indicated no differences in cytokine gene expression between control and exposure to BU. Data are presented as the mean ± SEM of three independent replicates.

A

	Signs	BU 24 h	BU 48 h	Damage Score	Control 24 hours	Control 48 hours	Damage
Epidermis	Hyperplasia	0	0	Null	0	0	Null
	Apoptosis	0	0	Null	0	0	Null
	Hyperkeratosis	0	0	Null	0	0	Null
	Hypergranulosis	0	0	Null	0	0	Null
	Parakeratosis	0	0	Null	0	0	Null
	Basal Damage	0	0	Null	0	0	Null
	Spongiosis	0	0	Null	1	1	Very Low
	Acantolysis	0	0	Null	0	0	Null
	Epidermal Detachment	1	1	Very Low	1 +/-0.3	1	Very low
	Epidermal Height (μm)	40.7 +/- 5.9	31 +/-6		67.5 +/- 3.88	74.9 +/-11.8	
Dermis	Infammatory infiltration	1	1	Low	1.3 +/-0.3	1	Low
	Edema	0	0	Low	0	0	Very Low
	Vascular congestion	0	0	Very Low	0	0	Very Low
	Hemorrhage	0	0	Very Low	0	0	Very Low
	Fibrosis	0	0	Very Low	0	0	Very Low
	Collagen degradation	0	0	Very Low	0.3	1	Very Low
	Myxoid degradation	0	0	Very Low	0	0	Very Low
	Granulocytic reaction	0	0	Very Low	0	0	Very Low

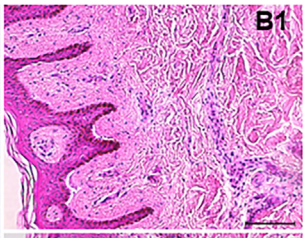

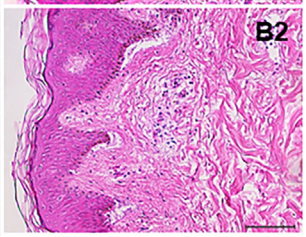

Escore	Level	Damage
0	0	Null
0-1	<25%	Very low
1-2	25%	Low
2-3	50%	Moderate
3-4	75%	Severe
4	>75%	Highly Severe

Fig. 7. Histological analysis of sections of human skin explants: (A) Data table of three explants per experimental condition showing signs and level of damage in histological sections of full thickness skin after BU or PBS (control) application. B) **Representative histological sections**, fixed and stained with hematoxylin-eosin, obtained from explants treated for 24 h with BU (B1) or PBS (B2). The scale bar represents 200 μm.

4. Conclusions

The experiments performed in this work revealed that the improved stability of imipenem in the BU NADES formulation correlates with an improvement in the antibacterial effectiveness of this drug. This finding is mainly supported by the arrangement of the BU in the solvation sphere of the drug, providing a close relation with betaine, the protective component. Added to this, the type of release unveiled by the kinetic analysis imprints a nonrestricted and fast drug release, promoting the observed improvement in the antibiotic activity against bacteria growing in planktonic and biofilm conditions. Furthermore, the favourable biosafety results presented herein for BU should promote further investigation on biomedical applications of carbapenem antibiotics.

Declaration of Competing Interest

The authors declare that they have no known competing financial interests or personal relationships that could have appeared to influence the work reported in this paper.

Acknowledgments

This work was supported by Concurso Interno de Investigación number 23400168 of Universidad del Desarrollo.

References

[1] By 2050, drug-resistant infections could cause global economic damage on par with 2008 financial crisis, (n.d.). https://www.worldbank.org/en/news/press-release/2016/09/18/by-2050-drug-resistant-infections-could-cause-global-economic-damage-on-par-with-2008-financial-crisis (accessed September 21, 2021).

[2] J. Brauers, S. Ewig, M. Kresken, beta-lactam-antibiotics in the treatment of community-acquired respiratory tract infections with penicillin-resistant pneumococci, Pneumologie 56 (2002) 605–609.

[3] M. Ibarra, M. Vázquez, P. Fagiolino, Current PBPK models: are they predicting tissue drug concentration correctly?, Drugs R D. 20 (2020) 295–299.

[4] C.O. Vrancianu, I. Gheorghe, E.-G. Dobre, I.C. Barbu, R.E. Cristian, M. Popa, S.H. Lee, C. Limban, I.M. Vlad, M.C. Chifiriuc, Emerging strategies to combat β-lactamase producing ESKAPE pathogens, Int. J. Mol. Sci. 21 (22) (2020) 8527, https://doi.org/10.3390/ijms21228527.

[5] A. Vermote, S. Van Calenbergh, Small-molecule potentiators for conventional antibiotics against staphylococcus aureus, ACS Infect Dis. 3 (11) (2017) 780–796.

[6] E. Speri, C. Kim, S. De Benedetti, Y. Qian, E. Lastochkin, J. Fishovitz, J.F. Fisher, S. Mobashery, Cinnamonitrile adjuvants restore susceptibility to β-lactams against methicillin-resistant staphylococcus aureus, ACS Med. Chem. Lett. 10 (8) (2019) 1148–1153.

[7] K.A. Rodvold, Pharmacodynamics of antiinfective therapy: taking what we know to the patient's bedside, Pharmacotherapy 21 (2001) 319S–330S.

[8] V.C. Cox, P.J. Zed, Once-daily cefazolin and probenecid for skin and soft tissue infections, Ann. Pharmacother. 38 (3) (2004) 458–463.

[9] J. Jackson, A.W. Fernandes, W. Nelson, A naturalistic comparison of amoxicillin/clavulanate extended release versus immediate release in the treatment of acute bacterial sinusitis in adults: a retrospective data analysis, Clin. Ther. 28 (2006) 1462–1471.

[10] M. Kono, N.K. Umar, S. Takeda, M. Ohtani, D. Murakami, H. Sakatani, F. Kaneko, D. Nanushaj, M. Hotomi, Novel antimicrobial treatment strategy based on drug delivery systems for acute otitis media, Front. Pharmacol. 12 (2021) 640514.

[11] P.N.A. Harris, P.A. Tambyah, D.C. Lye, Y. Mo, T.H. Lee, M. Yilmaz, T.H. Alenazi, Y. Arabi, M. Falcone, M. Bassetti, E. Righi, B.A. Rogers, S. Kanj, H. Bhally, J. Iredell, M. Mendelson, T.H. Boyles, D. Looke, S. Miyakis, G. Walls, M. Al Khamis, A. Zikri, A. Crowe, P. Ingram, N. Daneman, P. Griffin, E. Athan, P. Lorenc, P. Baker, L. Roberts, S.A. Beatson, A.Y. Peleg, T. Harris-Brown, D.L. Paterson, MERINO Trial Investigators and the Australasian Society for Infectious Disease Clinical Research Network (ASID-CRN), Effect of Piperacillin-Tazobactam vs Meropenem on 30-Day Mortality for Patients With E coli or Klebsiella pneumoniae Bloodstream Infection and Ceftriaxone Resistance: A Randomized Clinical Trial, JAMA. 320 (2018) 984–994.

[12] B. Olivares, F. Martínez, L. Rivas, C. Calderón, J.M. Munita, P.R. Campodonico, A natural deep eutectic solvent formulated to stabilize β-lactam antibiotics, Sci. Rep. 8 (2018) 14900.

[13] Y. Dai, J. van Spronsen, G.-J. Witkamp, R. Verpoorte, Y.H. Choi, Natural deep eutectic solvents as new potential media for green technology, Anal. Chim. Acta. 766 (2013) 61–68.

[14] R.W. Korsmeyer, R. Gurny, E. Doelker, P. Buri, N.A. Peppas, Mechanisms of solute release from porous hydrophilic polymers, Int. J. Pharm. 15 (1) (1983) 25–35.

[15] B.J. Kong, A. Kim, S.N. Park, Properties and in vitro drug release of hyaluronic acid-hydroxyethyl cellulose hydrogels for transdermal delivery of isoliquiritigenin, Carbohydr. Polym. 147 (2016) 473–481.

[16] Z. Liu, L.i. Li, S. Zhang, J. Lomeo, A. Zhu, J. Chen, S. Barrett, A. Koynov, S. Forster, P. Wuelfing, W. Xu, Correlative image-based release prediction and 3D microstructure characterization for a long acting parenteral implant, Pharm. Res. 38 (11) (2021) 1915–1929, https://doi.org/10.1007/s11095-021-03145-2.
[17] B.L. Price, A.M. Lovering, F.L. Bowling, C.B. Dobson, Development of a novel collagen wound model to simulate the activity and distribution of antimicrobials in soft tissue during diabetic foot Infection, Antimicrob. Agents Chemother. 60 (11) (2016) 6880–6889.
[18] M. Werthén, L. Henriksson, P.Ø. Jensen, C. Sternberg, M. Givskov, T. Bjarnsholt, An in vitro model of bacterial infections in wounds and other soft tissues, APMIS 118 (2) (2010) 156–164.
[19] M.E. Lund, J. To, B.A. O'Brien, S. Donnelly, The choice of phorbol 12-myristate 13-acetate differentiation protocol influences the response of THP-1 macrophages to a pro-inflammatory stimulus, J. Immunol. Methods. 430 (2016) 64–70.
[20] C. Oses, B. Olivares, M. Ezquer, C. Acosta, P. Bosch, M. Donoso, P. Léniz, F. Ezquer, Preconditioning of adipose tissue-derived mesenchymal stem cells with deferoxamine increases the production of pro-angiogenic, neuroprotective and anti-inflammatory factors: potential application in the treatment of diabetic neuropathy, PLoS One 12 (2017) e0178011.
[21] J.J.L. Jacobs, C. Lehé, K.D.A. Cammans, P.K. Das, G.R. Elliott, An in vitro model for detecting skin irritants: methyl green-pyronine staining of human skin explant cultures, Toxicol. In Vitro 16 (2002) 581–588.
[22] Polymers through noncovalent bonding, AccessScience. (2015). https://doi.org/
[23] W.W. Hauck, V.P. Shah, S.W. Shaw, C.T. Ueda, Reliability and reproducibility of vertical diffusion cells for determining release rates from semisolid dosage forms, Pharm. Res. 24 (11) (2007) 2018–2024.
[24] I. Kanfer, S. Rath, P. Purazi, N.A. Mudyahoto, In vitro release testing of semi-solid dosage forms, Dissolution Technol. 24 (3) (2017) 52–60.
[25] K. Kosmidis, E. Rinaki, P. Argyrakis, P. Macheras, Analysis of Case II drug transport with radial and axial release from cylinders, Int. J. Pharm. 254 (2) (2003) 183–188.
[26] N.L. Thomas, A.H. Windle, A theory of case II diffusion, Polymer. 23 (4) (1982) 529–542.
[27] A.W. Hixson, J.H. Crowell, Dependence of reaction velocity upon surface and agitation, Indus. Eng. Chem. 23 (10) (1931) 1160–1168, https://doi.org/10.1021/ie50262a025.
[28] A.E. Hafeman, K.J. Zienkiewicz, E. Carney, B. Litzner, C. Stratton, J.C. Wenke, S.A. Guelcher, Local delivery of tobramycin from injectable biodegradable polyurethane scaffolds, J. Biomater. Sci. Polym. Ed. 21 (1) (2010) 95–112.
[29] S.V. Efimov, I.A. Khodov, E.L. Ratkova, M.G. Kiselev, S. Berger, V.V. Klochkov, Detailed NOESY/T-ROESY analysis as an effective method for eliminating spin diffusion from 2D NOE spectra of small flexible molecules, J. Mol. Struct. 1104 (2016) 63–69.
[30] F. Pedinielli, J.-M. Nuzillard, P. Lameiras, Mixture analysis in viscous solvents by NMR spin diffusion spectroscopy: viscY. application to high- and low-polarity organic compounds dissolved in sulfolane/water and sulfolane/DMSO-d6 blends, Anal. Chem. 92 (7) (2020) 5191–5199, https://doi.org/10.1021/acs.analchem.9b05725.
[31] P.L. Turgeon, C. Desrochers, Stability of imipenem in Mueller-Hinton agar stored at 4 degrees C, Antimicrob. Agents Chemother. 28 (5) (1985) 711–712.
[32] D.J. Nickolai, C.J. Lammel, B.A. Byford, J.H. Morris, E.B. Kaplan, W.K. Hadley, G.F. Brooks, Effects of storage temperature and pH on the stability of eleven beta-lactam antibiotics in MIC trays, J. Clin. Microbiol. 21 (3) (1985) 366–370.
[33] D.J. Swanson, C. DeAngelis, I.L. Smith, J.J. Schentag, Degradation kinetics of imipenem in normal saline and in human serum, Antimicrob. Agents Chemother. 29 (5) (1986) 936–937.
[34] G.L. Drusano, H.C. Standiford, C. Bustamante, A. Forrest, G. Rivera, J. Leslie, B. Tatem, D. Delaportas, R.R. MacGregor, S.C. Schimpff, Multiple-dose pharmacokinetics of imipenem-cilastatin, Antimicrob. Agents Chemother. 26 (5) (1984) 715–721.
[35] N. Høiby, H. Krogh Johansen, C. Moser, Z. Song, O. Ciofu, A. Kharazmi, Pseudomonas aeruginosa and the in vitroand in vivo biofilm mode of growth, Microbes Infect. 3 (1) (2001) 23–35.
[36] Clsi, Performance Standards for Antimicrobial Susceptibility Testing; Twenty-Seventh Edition, 2017
[37] W. Hengzhuang, H. Wu, O. Ciofu, Z. Song, N. Høiby, Pharmacokinetics/pharmacodynamics of colistin and imipenem on mucoid and nonmucoid Pseudomonas aeruginosa biofilms, Antimicrob. Agents Chemother. 55 (9) (2011) 4469–4474.
[38] E. Werner, F. Roe, A. Bugnicourt, M.J. Franklin, A. Heydorn, S. Molin, B. Pitts, P.S. Stewart, Stratified growth in Pseudomonas aeruginosa biofilms, Appl. Environ. Microbiol. 70 (10) (2004) 6188–6196.
[39] M. Stasiulewicz, A. Panuszko, M. Śmiechowski, P. Bruździak, P. Maszota, J. Stangret, Effect of urea and glycine betaine on the hydration sphere of model molecules for the surface features of proteins, J. Mol. Liq. 324 (2021) 115090.
[40] The effects of urea and n-propanol on collagen denaturation: using DSC, circular dicroism and viscosity, Thermochim. Acta. 409 (2004) 201–206
[41] M. Hayyan, C.Y. Looi, A. Hayyan, W.F. Wong, M.A. Hashim, G. Papaccio, In Vitro and In Vivo toxicity profiling of ammonium-based deep eutectic solvents, PLoS One 10 (2) (2015) e0117934, https://doi.org/10.1371/journal.pone.0117934.
[42] I.P.E. Macário, H. Oliveira, A.C. Menezes, S.P.M. Ventura, J.L. Pereira, A.M.M. Gonçalves, J.A.P. Coutinho, F.J.M. Gonçalves, Cytotoxicity profiling of deep eutectic solvents to human skin cells, Sci. Rep. 9 (2019) 3932.
[43] Y.P. Mbous, M. Hayyan, W.F. Wong, C.Y. Looi, M.A. Hashim, Unraveling the cytotoxicity and metabolic pathways of binary natural deep eutectic solvent systems, Sci. Rep. 7 (2017) 41257.
[44] K. Radošević, M. Cvjetko Bubalo, V. Gaurina Srček, D. Grgas, T. Landeka Dragičević, I. Radojčić Redovniković, Evaluation of toxicity and biodegradability of choline chloride based deep eutectic solvents, Ecotoxicol. Environ. Saf. 112 (2015) 46–53.
[45] X.-D. Hou, Q.-P. Liu, T.J. Smith, N. Li, M.-H. Zong, V. Bansal, Evaluation of toxicity and biodegradability of cholinium amino acids ionic liquids, PLoS One 8 (3) (2013) e59145, https://doi.org/10.1371/journal.pone.0059145.
[46] K. Radošević, J. Železnjak, M. Cvjetko Bubalo, I. Radojčić Redovniković, I. Slivac, V., Gaurina Srček, Comparative in vitro study of cholinium-based ionic liquids and deep eutectic solvents toward fish cell line, Ecotoxicol. Environ. Saf. 131 (2016) 30–36.
[47] N. Gal, D. Malferrari, S. Kolusheva, P. Galletti, E. Tagliavini, R. Jelinek, Membrane interactions of ionic liquids: possible determinants for biological activity and toxicity, Biochim. Biophys. Acta. 2012 (1818) 2967–2974.
[48] K.O. Evans, Room-temperature ionic liquid cations act as short-chain surfactants and disintegrate a phospholipid bilayer, Colloids Surf. A Physicochem. Eng. Asp. 274 (1-3) (2006) 11–17.
[49] F. Jesus, H. Passos, A.M. Ferreira, K. Kuroda, J.L. Pereira, F.J.M. Gonçalves, J.A.P. Coutinho, S.P.M. Ventura, Zwitterionic compounds are less ecotoxic than their analogous ionic liquids, Green Chem. 23 (10) (2021) 3683–3692.
[50] B.-Y. Zhao, P. Xu, F.-X. Yang, H. Wu, M.-H. Zong, W.-Y. Lou, Biocompatible Deep Eutectic Solvents Based on Choline Chloride: Characterization and Application to the Extraction of Rutin from Sophora japonica, ACS Sustainable Chem. Eng. 3 (2015) 2746–2755.
[51] W. Chanput, M. Reitsma, L. Kleinjans, J.J. Mes, H.F.J. Savelkoul, H.J. Wichers, β-Glucans are involved in immune-modulation of THP-1 macrophages, Mol. Nutr. Food Res. (2012) n/a–n/a, https://doi.org/10.1002/mnfr.1734.
[52] A. Peramo, C.L. Marcelo, S.A. Goldstein, D.C. Martin, Novel organotypic cultures of human skin explants with an implant-tissue biomaterial interface, Ann. Biomed. Eng. 37 (2) (2009) 401–409.
[53] T. Agner, An experimental study of irritant effects of urea in different vehicles, Acta Derm. Venereol. Suppl. 177 (1992) 44–46.